THE PLANING TOOL'S PROFILING FOR ROOTS COMPRESSOR'S ROTORS. GRAPHICAL METHOD IN CATIA

Nicuşor Baroiu, Virgil Gabriel Teodor, Florin Susac, Viorel Păunoiu, Nicolae Oancea

"Dunărea de Jos" University of Galați, Department of Manufacturing Engineering,
Domnească Street, No. 111, 800201, Galați, România

Corresponding author: Virgil Gabriel Teodor, virgil.teodor@ugal.ro

Abstract: The helical surfaces with a very large pitch can not be machined by turning with profiled tools. For this reason, in case of this worm's types, especially for small machining batch or for reparations, the machining with single edge cutting tools it is preferred. These tools have the advanced to be less expensive and easy to manufacture compared with the side mill tools. The planing tool's profiling assumes to determine which cylindrical surface is reciprocally enwrapping with the helical surface to be generated. The general profiling method uses the fundamental theorem of Litvin for surface enveloping. Meanwhile, some analytical theorems were developed as complementary methods for study the contact between a helical surface and a cylindrical one. A method for determination of the planing tool is presented in this paper. The method is developed in CATIA design environment, based on a complementary analytical method for study of enwrapping surfaces, the method of "relative generating trajectories". A graphical application for a Roots compressor rotor is presented. The results are compared with those obtained by an analytical method. It is highlighted the obviously difficulty involved by the equations handling in case of analytical method.

Key words: non-analytical method, CATIA, planing tool, compressor rotors

1. INTRODUCTION

The tools for planning cylindrical helical surfaces with constant pitch generate a cylindrical surface.
Usually, the generatrix of this surface is tangent to the helix with maximum radius. The planing tool's profiling assumes determining of a cylindrical surface reciprocally enwrapping with the helical surface to be generated [1, 2]. The general profiling method calls the fundamental theorem of the surfaces enwrapping [1]. Analytical complementary theorems for study of the contact between a helical surface and a cylindrical one were elaborated by Oancea [2] and Teodor [3].
The specialty literature concerning about this issue. Petukhov [5] analytical deals with template machining precision for checking of helical surfaces generated with side mill, establishing the form and values of generating errors according to the tool's position regarding the generated helical surface. Petukhov [6] approach the influence of the tool's back face form on the cutting edge precision and, also, on the generated helical surface precision. New mathematical models for tool's profiling are presented by Kiryutin [7]. The development of design graphical environments allows developing some specific methods for profiling of these tools' types, Berbinschi et al., [4]. A specific algorithm developed in CATIA based on a new method for determining the relative generating trajectories is presented in this paper. The algorithm allows profiling the planing tool's cylindrical surface reciprocally enwrapping with a helical surface with constant pitch. Numerical applications for Roots helical rotors are also presented.

2. THE "RELATIVE GENERATING TRAJECTORIES" METHOD

In order to apply the relative generating trajectories method for profiling the cylindrical tool reciprocally enveloping with a cylindrical helical surface with constant pitch we use the reference system presented in Figure 1. There are defined:
- the model of the helical surface to be generated, with the helical flank $\sum$;
- the $\vec{t}$ direction of the cylindrical surface's generatrix (planing tool) parallels to the tangent at the helical line belongs to the external cylinder of the helical surface with radius R_e;
- the unfold helical line corresponding to the cylinder with the radius R_e.
The helix has helical parameter p.
The reference systems are defined:
- XYZ is the reference system associated with the helical surface $\sum$. The Z axis is the axis of helix.
- $X_1Y_1Z_1$ - reference system associated with the conjugated cylindrical surface, with Z_1 axis overlapped to the $\vec{t}$ direction;
- xyz - global reference system.

The angle between the helix axis, $\vec{V}$ (Z), and the tangent to the helix with radius R_e is denoted with α:

$$\tan\alpha = \frac{2\cdot\pi\cdot R_e}{2\cdot\pi\cdot p} = \frac{R_e}{p} \qquad (1)$$

with p helical parameter of the helical surface. We notice that the axes X and X_1, Figure 1, of the two reference systems have the same direction and sense - the normal direction to the helix axis, $\vec{V}$.

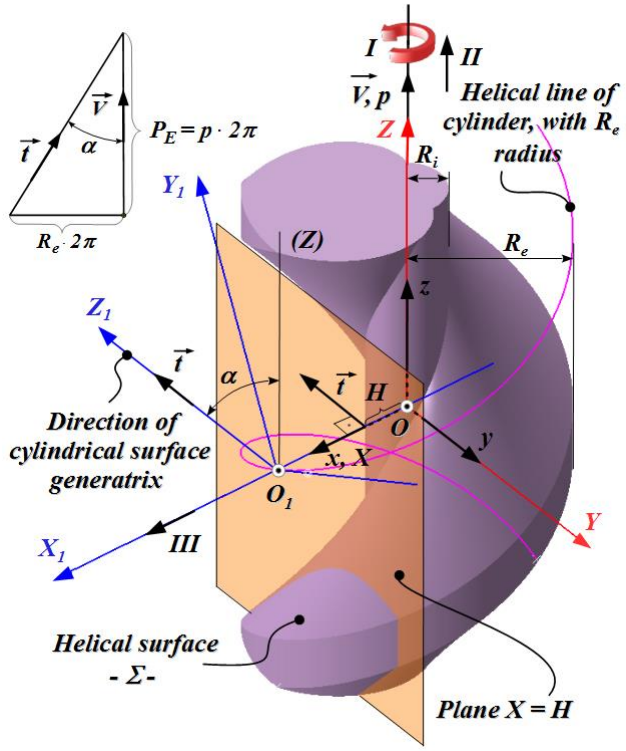

Fig. 1. The ∑ helical surface; reference systems; the directrix of the cylindrical surface

The kinematics of the generation process with planing tool includes the movements, see Figure 1:
- the assembly of movements *I* and *II*, rotation and translation of the helical surface around the *V* axis and, correlated, along the same axis - the helical movement *V*, *p* during which the ∑ surface is self generated;
- the rectilinear movement *III* along the $\vec{t}$ generatrix, made by the cylindrical tool (the planing tool, not represented in figure). The helical surface ∑ and the cylindrical surface with generatrix $\vec{t}$, the tool's surface *S*, are reciprocally enveloping surfaces in this movements assembly. According to the relative generating trajectories method, the contact between planes profiles of the ∑ and *S* surfaces is analysed in the relative movement of the surfaces - movements previously defined. Let be the ∑ helical surface defined in the *XYZ* reference system, in form:

$$\Sigma\begin{cases} X = X(u,v); \\ Y = Y(u,v); \\ Z = Z(u,v), \end{cases} \qquad (2)$$

with *u* and *v* independent variables parameters.
The plane

$$X = H \qquad (3)$$

is considered with *H* arbitrary variable. This plane is orthogonal to the *X* axis, see Figure 1, with

$$R_i \le H \le R_e \qquad (4)$$

In principle, the intersection of the plane (3) with the surface ∑, Figure 1, is a curve on form:

$$(C_\Sigma)_H \begin{cases} X = H; \\ Y = Y(u); \\ Z = Z(u), \end{cases} \qquad (5)$$

if is accepted the equivalence of (3) condition as link between the *u* and *v* parameters,

$$v = v(u). \qquad (6)$$

The relative trajectories of curves $(C_\Sigma)_H$, regarding the future cylindrical surface *S*, in the movements assembly (*I*, *II*, *III*), for *H* variable, will determine the form of the primary peripheral surface of the cylindrical tool. Since the helical surface ∑ is self-generates in the assembly of movements (*I*, *II*) the surface's characteristic will not depends by these movements. The only movement which will determine the surface's characteristic is the translation along the $\vec{t}$ generatrix of the future cylindrical tool.
In this way, the problem is considerably simplified, reducing to the determination of the tangency point between the $(C_\Sigma)_H$ curve and the generatrix of the future *S* surface, in each plane *X* = *H*. The cylindrical surface admit as directrix the $\vec{t}$ versor,

$$\vec{t} = -\sin\alpha\cdot\vec{j} - \cos\alpha\cdot\vec{k} \qquad (7)$$

The tangent to the $(C_\Sigma)_H$ curve is defined starting from the equations (5). Let be $(\vec{T}_\Sigma)_H$ this tangent:

$$(\vec{T}_\Sigma)_H = -\dot{Z}_u\cdot\vec{j} + \dot{Y}_u\cdot\vec{k} \qquad (8)$$

From the condition that the two directions, $\vec{t}$ and $\left(\vec{T}_\Sigma\right)_H$, have to be identical, results:

$$\begin{aligned} -\dot{Z}_u &= -\sin\alpha; \\ \dot{Y}_u &= -\cos\alpha, \end{aligned} \tag{9}$$

from where results the condition for determining the point onto $\left(C_\Sigma\right)_H$ where the tangent to this is parallel with $\vec{t}$,

$$\tan\alpha = \frac{-\dot{Z}_u}{\dot{Y}_u}. \tag{10}$$

The (5) and (10) equations assembly represents, in the *H* plane, the coordinates of the tangency point with the generatrix of the future cylindrical surface *S*. In principle, the equations of the characteristic curve $C_{\Sigma,H}$ are in form:

$$C_{\Sigma,S}\begin{vmatrix} X = H; \\ Y = Y\left(u_H\right); \\ Z = Z\left(u_H\right), \end{vmatrix} \tag{11}$$

for *H* variable and u_H the particular value of the *u* parameter which accomplish, in each plane $X = H$, the condition (10).
The analytical model of the *S* cylindrical surface is obtained starting from the equations (11), see Figure 2, in form:

$$S\begin{vmatrix} X = H; \\ Y = Y\left(u_H\right) - \lambda\cdot\sin\alpha; \\ Z = Z\left(u_H\right) - \lambda\cdot\cos\alpha, \end{vmatrix} \tag{12}$$

with λ variable scalar parameter.

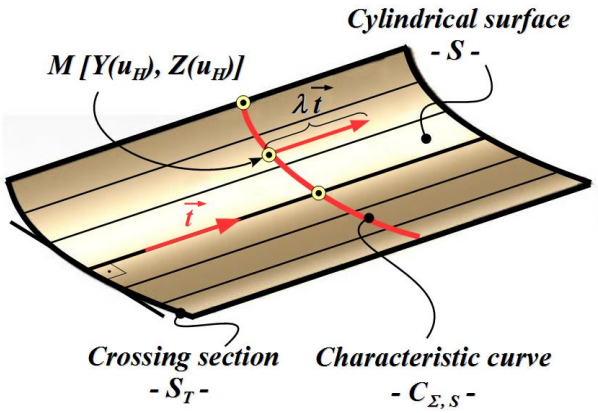

Fig. 2. *S* cylindrical surface and its crossing section

The crossing section of the cylindrical surface is obtained from (12) by intersecting the *S* surface with plane, Figure 2:

$$Z_1 = 0, \tag{13}$$

For this, is necessary to consider the coordinates transformation

$$X_1 = \omega_1(\alpha)\cdot\left[X - a\right] \tag{14}$$

where:

$$\omega_1(\alpha) = \begin{pmatrix} 1 & 0 & 0 \\ 0 & \cos\alpha & \sin\alpha \\ 0 & -\sin\alpha & \cos\varepsilon \end{pmatrix};\ a = \begin{pmatrix} R_e \\ 0 \\ 0 \end{pmatrix}, \tag{15}$$

with the α defined by (1).
From (12) and (14) results the form of the cylindrical surface in the $X_1Y_1Z_1$ reference system, see Figure 2:

$$\begin{aligned} \begin{pmatrix} X_1 \\ Y_1 \\ Z_1 \end{pmatrix} &= \begin{pmatrix} 1 & 0 & 0 \\ 0 & \cos\alpha & \sin\alpha \\ 0 & -\sin\alpha & \cos\alpha \end{pmatrix}\cdot \\ &\cdot\left[\begin{pmatrix} H \\ Y\left(u_H\right) - \lambda\cdot\sin\alpha \\ Z\left(u_H\right) - \lambda\cdot\cos\alpha \end{pmatrix} - \begin{pmatrix} R_e \\ 0 \\ 0 \end{pmatrix}\right] \end{aligned} \tag{16}$$

in principle:

$$\begin{vmatrix} X_1 = H - R_e; \\ Y_1 = Y_1\left(u_H, \lambda\right); \\ Z_1 = Z\left(u_H, \lambda\right). \end{vmatrix} \tag{17}$$

From (17), eliminating the λ parameter from equation (13), the crossing section form results:

$$\begin{vmatrix} X_1 = H - R_e; \\ Y_1 = Y_1\left(u\right); \\ Z_1 = 0. \end{vmatrix} \tag{18}$$

The form (18) allows drawing the physical or virtual template for check the cutting edge of the panning tool which generate, in the rectilinear movement along the $\vec{t}$ direction, the *S* cylindrical surface, Figure 3.

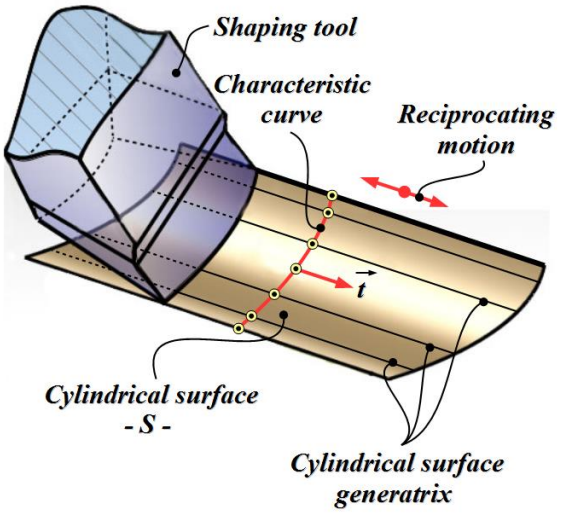

Fig. 3. Planing tool's profile and characteristic curve

3. GRAPHICAL METHOD IN CATIA

A graphical solution was developed in CATIA design environment.

The profiling algorithm for the planning tool, assumes the 3D modeling of the surface to be generated, $\sum$, and the generation of the reference systems: *XYZ* as the reference system associated with the helical surface $\sum$; $X_1Y_1Z_1$, reference system associated with the conjugated cylindrical surface and *xyz*, global reference system. Consequently, a plane characterized by the cote $X = H$ is generated. Intersecting (*INTERSECTION* command) this plane with the $\sum$ helical surface is obtained the curve $(C_\Sigma)_H$. One of the points belonging to this curve will belongs also to the characteristic curve. This point is the tangency point between the $C_\Sigma)_H$ curve and a straight line with direction given by the $\vec{t}$ versor. The point is obtained drawing a line parallel with $\vec{t}$ versor and constraint it to be tangent (*TANGENCY* constrints) to the intersection curve $(C_\Sigma)_H$. In this way, a suite of points onto the characteristic curve are determined. The characteristic curve is determined drawing a spline which admits as control points the previously determined points. The surface of the future planning tools is determined generating with *SWEEP* command a surface which admit as generatrix the characteristic curve and as directrix the $\vec{t}$ direction.

The crossing section of the planning tool is obtained intersectin the surface of tool with a plane perpenducilar to the helical line.

4. APPLICATIONS — PLANNING TOOL FOR A SCREW ROOTS COMPRESSOR

The Roots compressors can be included helical worms with coarse pitch, with cycloid crossing profile, see Figure 4.

They are defined the reference systems:

xyz is the global reference system with *z* axis joined with the axis of the cycloid worm;

$x_0y_0z_0$ - auxiliary reference system with z_0 axis joined with the rotation axis of the roulette;

XYZ - mobile reference system, with *Z* axis overlapped to the *z* axis and joined with the basis with radius *Rr*;

$X_2Y_2Z_2$ - mobile reference system joined with the roulette with radius *r*.

The crossing section of the cycloid worm is a profile composed from an curves' assembly: epicycloids, generated by a point onto the roulette with radius *r*, which rolls without sliding onto the base curve with radius *R* $\left(BC\right)$ and hypocycloid with the same roulette and base curve $\left(AB\right)$.

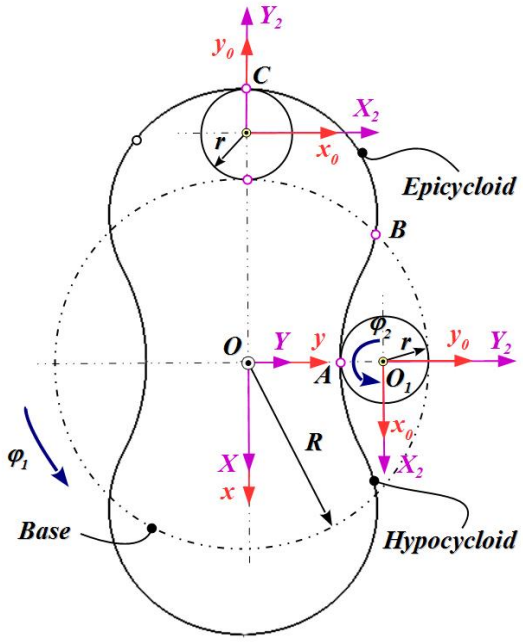

Fig. 4. Crossing section of the cycloid worm; reference systems

In the X_2Y_2reference system, the roulette equation is on form:

$$\begin{vmatrix} X_2 = r \cdot \cos\theta; \\ Y_2 = r \cdot \sin\theta, \end{vmatrix} \quad (19)$$

with θ variable parameter, for the current point onto the roulette with radius *r*.

In the rolling process of the roulette with radius *r*, with base curve with radius *R*, let be φ_1 and φ_2 the movement parameters which respects the condition

$$R \cdot \varphi_1 = r \cdot \varphi_2. \quad (20)$$

The generating movements, regarding the global reference system *xy*, are:

$$x = \omega_3^T(\varphi_1)\cdot X \quad \text{base curve rotation;} \tag{21}$$

$$x_0 = \omega_3^T(\varphi_2)\cdot X_2 \quad \text{roulette curve rotation} \tag{22}$$

if the x_0y_0 reference system is joined with the roulette center, the link between the xy global reference system and the x_0y_0 relative reference system is:

$$x = x_0 - a;\ a = \begin{pmatrix} 0 \\ -(R-r) \end{pmatrix} \tag{23}$$

From (21), (22) and (23) results:

$$\omega_3^T(\varphi_1)X = \omega_3^T(\varphi_2)X_2 - a \tag{24}$$

The profile of the *AB* section results:

$$AB\begin{vmatrix} X = r\cdot\cos(\varphi_2+\theta-\varphi_1)+(R-r)\cdot\sin\varphi_1; \\ Y = r\cdot\sin(\varphi_2+\theta-\varphi_1)+(R-r)\cdot\cos\varphi_1. \end{vmatrix} \tag{25}$$

The equations (25), for $\theta = -\frac{\pi}{2}$, representing the *A* point from the roulette is determined the hypocycloid curve *AB* onto the worm's frontal profile:

$$AB\begin{vmatrix} X = r\cdot\cos\left(\varphi_2-\varphi_1-\frac{\pi}{2}\right)+(R-r)\cdot\sin\varphi_1 \\ Y = r\cdot\sin\left(\varphi_2-\varphi_1-\frac{\pi}{2}\right)+(R-r)\cdot\cos\varphi_1 \end{vmatrix} \tag{26}$$

or

$$AB\begin{vmatrix} X = r\cdot\sin(\varphi_2-\varphi_1)+(R-r)\cdot\sin\varphi_1; \\ Y = -r\cdot\cos(\varphi_2-\varphi_1)+(R-r)\cdot\cos\varphi_1. \end{vmatrix} \tag{27}$$

Usually $r = \frac{R}{4}$, therefore:

$$\varphi_2 = \frac{R}{r}\cdot\varphi_1 = 4\cdot\varphi_1. \tag{28}$$

Similarly, the BC arc's profile is determined.
In position $\theta = \pi/2$ the senses of rotation movements of base and roulette are opposite. The transformation (24) is modified in form:

$$\omega_3^T(\varphi_1)\cdot X = \omega_3^T(-\varphi_2)\cdot X_1 - \begin{pmatrix} 0 \\ -(R+r) \end{pmatrix} \tag{29}$$

From (29) results:

$$\begin{pmatrix} X \\ Y \end{pmatrix} = \begin{pmatrix} \cos\varphi_1 & \sin\varphi_1 \\ -\sin\varphi_1 & \cos\varphi_1 \end{pmatrix}\cdot$$
$$\cdot\left[\begin{pmatrix} \cos\varphi_2 & \sin\varphi_2 \\ -\sin\varphi_2 & \cos\varphi_2 \end{pmatrix}\cdot\begin{pmatrix} r\cdot\cos\theta \\ r\cdot\sin\theta \end{pmatrix} - \begin{pmatrix} 0 \\ -(R+r) \end{pmatrix}\right] =$$
$$= \begin{pmatrix} \cos\varphi_1 & \sin\varphi_1 \\ -\sin\varphi_1 & \cos\varphi_1 \end{pmatrix}\cdot\begin{pmatrix} r\cdot\cos(\varphi_2-\theta) \\ -r\cdot\sin(\varphi_2-\theta)+(R+r) \end{pmatrix} \tag{30}$$

$$BC\begin{vmatrix} X = r\cdot\cos(\varphi_1+\varphi_2-\theta)+(R+r)\cdot\sin\varphi_1; \\ Y = -r\cdot\sin(\varphi_1+\varphi_2-\theta)+(R+r)\cdot\cos\varphi_1. \end{vmatrix} \tag{31}$$

For $\theta = \frac{\pi}{2}$ (the *C* point onto the circle with *r* radius), results the profile of epicycloids *BC*:

$$BC\begin{vmatrix} X = r\cdot\sin(\varphi_1+\varphi_2)+(R+r)\cdot\sin\varphi_1; \\ Y = r\cdot\cos(\varphi_1+\varphi_2)+(R+r)\cdot\cos\varphi_1. \end{vmatrix} \tag{32}$$

The assembly of the cycloid arcs AB and BC forms the half of the crossing profile of compressor rotor.
As results from (28),

$$\varphi_1+\varphi_2 = \varphi_1+4\cdot\varphi_1 = 5\cdot\varphi_1 \tag{33}$$

Though the equations of the worm's frontal profile are in form:

$$AB\begin{vmatrix} X = r\cdot\sin(3\cdot\varphi_1)+(R-r)\cdot\sin\varphi_1; \\ Y = -r\cdot\cos(3\cdot\varphi_1)+(R-r)\cdot\cos\varphi_1, \end{vmatrix} \tag{34}$$

respectively

$$BC\begin{vmatrix} X = r\cdot\sin(5\cdot\varphi_1)+(R+r)\cdot\sin\varphi_1; \\ Y = r\cdot\cos(5\cdot\varphi_1)+(R+r)\cdot\cos\varphi_1. \end{vmatrix} \tag{35}$$

For the AB cycloid arc, the variation limit of the φ_1 angle is deduced from the condition

$$X^2+Y^2 = R^2 \tag{36}$$

with *x* and *y* from (34) and (35):

$$r^2+(R-r)^2-\sin(3\varphi_1+\varphi_1) = R^2-2r\cdot(R-r) \tag{37}$$

or

$$-R^2+r^2+(R-r)^2=(R-r)\cdot\sin(4\cdot\varphi_1) \qquad (38)$$

Results

$$\varphi_1=\arcsin\left[\frac{(R-r)^2+r^2-R^2}{2\cdot r\cdot(R-r)}\right] \qquad (39)$$

Similarly is made the calculus for BC.
The two half profiles of the rotor's frontal section are presented in Figure 4. Obviously, for symmetry sake the frontal composed profile is obtained.
The worm's helical flank is obtained from (34) and (35), by transforming

$$X=\omega_3^T(\varphi)\cdot X_{AB,BC}+p\cdot\psi\cdot\vec{k}, \qquad (40)$$

with ψ angular parameter of the helical motion and p helical parameter (clockwise worm). For an helix tilt angle of β = 15° on the external diameter of the worm, the helical parameter is

$$p=\frac{R+r}{\tan\beta}=\frac{R+r}{\tan 15^\circ}. \qquad (41)$$

So, the helical half-flanks have the equations:

- for the AB flank:

$$\begin{pmatrix}X\\Y\\Z\end{pmatrix}=\begin{pmatrix}\cos\psi & -\sin\psi & 0\\ \sin\psi & \cos\psi & 0\\ 0 & 0 & 1\end{pmatrix}\cdot \begin{pmatrix}r\cdot\sin(3\cdot\varphi_1)+(R-r)\cdot\sin\varphi_1\\ -r\cdot\cos(3\cdot\varphi_1)+(R-r)\cdot\cos\varphi_1\\ 0\end{pmatrix}+\begin{pmatrix}0\\0\\p\cdot\psi\end{pmatrix}, \qquad (42)$$

$$\Sigma_{AB}\begin{vmatrix}X=r\sin(\psi+3\varphi_1)+(R-r)\cdot\sin(\psi+\varphi_1);\\ Y=r\cos(\psi+5\varphi_1)+(R-r)\cdot\cos(\psi+\varphi_1);\\ Z=p\psi,\end{vmatrix} \qquad (43)$$

and, similarly, for the BC flank:

$$\Sigma_{BC}\begin{vmatrix}X=r\sin(\psi+5\varphi_1)+(R+r)\sin(\psi+\varphi_1);\\ Y=r\cos(\psi+5\varphi_1)+(R+r)\cos(\psi+\varphi_1);\\ Z=p\psi.\end{vmatrix} \qquad (44)$$

According to the presented algorithm, the in-plane section is determined with a variable plane, perpendicularly to the Y axis, see Figure 5.
For the flank with AB generatrix, the section with the plane $Y = H$ (H variable) is calculated:

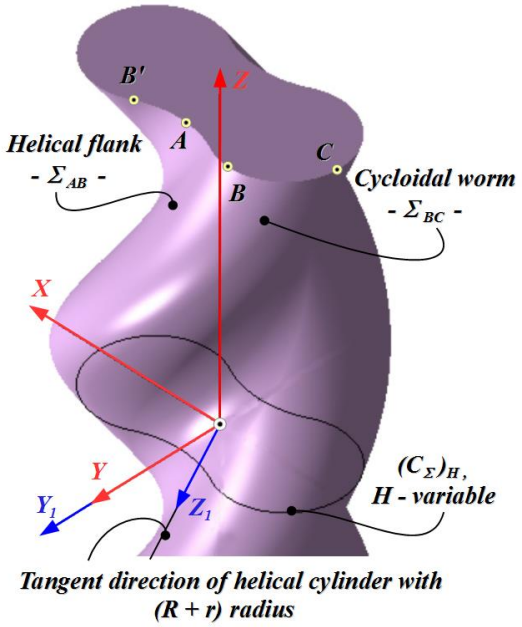

Fig. 5. Helical flanks, references systems

$$-r\cdot\cos(\psi+3\cdot\varphi_1)-(R-r)\cdot\cos(\psi-\varphi_1)=H \qquad (45)$$

A numerical dependency on form $\psi=\psi(\varphi_1)$ is determined for the variation of φ_1 angle between limits:

$$-\arcsin\left[\frac{(R-r)^2+r^2-R^2}{2\cdot r\cdot(R-r)}\right]<\varphi_1<\arcsin\left[\frac{(R-r)^2+r^2-R^2}{2\cdot r\cdot(R-r)}\right], \qquad (46)$$

for the $B'AB$ zone.
The analytical solution follows the previous methodology but it is obviously the difficulty to handle the equations of the helical surface.
Appling the graphical method developed in CATIA (see section 3), it was obtained the crossing section of the planning tool.
The coordinate of crossing section corresponding to various zones of the profile are given in Table 1, and the form of profile is presented in Figure 6.

Table 1. Coordinates of points on the crossing section of planning tool

Crt. no.	C'B'		B'B		BC	
	X [mm]	Y [mm]	X [mm]	Y [mm]	X [mm]	Y [mm]
1	-74.99	69.008	-49.90	34.78	-50.00	-34.79
2	-73.61	59.329	-31.09	20.95	-55.76	-36.53
3	-68.92	48.623	-25.00	0	-66.98	-45.85
4	-60.61	39.602	-29.66	-18.50	-71.63	-53.85
5	-50.00	34.790	-49.90	-34.78	-74.99	-69.00

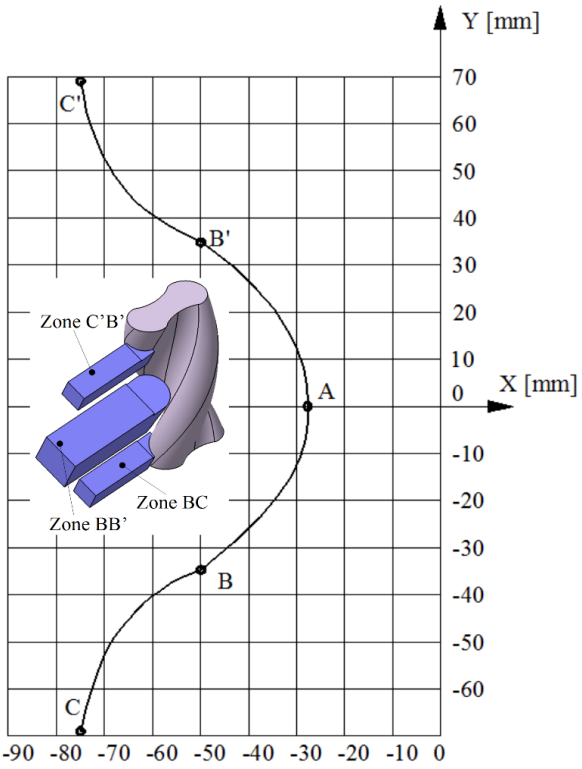

Fig. 6. Profile of planning tool

5. CONCLUSIONS

The graphical method developed in CATIA using the program commands allows a rigorous description of the 3D model of helical surface. Also, the intersection curves of the helical surfaces with the orthogonal planes of generatrix of the planning tool and the relative generating trajectories can be rigorous described.

The verification of the graphical solution with an analytical one can be made in the direct way using the coordinates of the characteristic curve, graphical determined, for calculation of the analytical condition. Theoretically, this value should be zero.

6. ACKNOWLEDGEMENTS

This work was supported by a grant of the Romanian National Authority for Scientific Research and Innovation, CNCS – UEFISCDI, project number PN-II-RU-TE-2014-4-0031.

7. REFERENCES

1. Litvin, F.L., (1984). *Theory of Gearing*, Reference Publication, 1212, NASA, Scientific and Technical Information Division, Washington D.C.

2. Oancea, N., (2004). *Generarea suprafeţelor prin înfăşurare (Surfaces generation through winding),* Vol. I-III, Galati University Press.

3. Teodor, V., Păunoiu, V., Berbinschi, S., Baroiu, N., Oancea, N., (2015). *The Metod of "In-Plane Generating Trajectories" for Tools which Generate by Enveloping - Application in CATIA*, Journal of Machine Engineering, 15(4), 69-80.

4. Berbinschi, S. et al., (2012). *3D Graphical Method for Profiling Tools that Generate Helical Surfaces*, International Journal of Advanced Manufacturing Technology, 60, 505-512.

5. Petukhov, Yu.E., Domnin, P.V., (2011). *Shaping in Machining a Screw Surfaces*, Rusian Engineering Research, 31(10), 1013-1015.

6. Petukhov, Yu.E., Movsesyan, A.V., (2007). *Determining of Shape of the Back Surface of Disc Milling Cutter for Machining a Contoured Surface*, Rusian Engineering Research, 22(8), 519-521.

7. Kiryutin, A.S., (2014). *Mathematical Model of Profiling Cutter Tools*, Scientific and Practical Journal "Modern scientific Researches and Innovations", 10.

8. Baroiu, N., Teodor, V., Oancea, N., (2015). *A new form of plane trajectories theorem. Generation with rotary cutters*, Bulletin of the Polytechnic Institute of Iaşi, LXI (LXV), Machine Construction, 27-36.

9. Cenk, M., Mümin, Ş., Mehmet, C., (2017). *The Effects on Surface Roughness of Parameters in Machining*, International Journal of Modern Manufacturing Technologies, ISSN 2067-3604, IX(1), 35-40.

10. Pruteanu, O., Cărăuşu, C., (2017), *The Influence of the Technological Parameters on the Superfinishing with the Abrasive Belt*, International Journal of Modern Manufacturing Technologies, ISSN 2067-3604, IX(1), 73-78.

11. Gheorghiţă, C., Gheorghiţă, V., (2015), *Application of Multiobjective Methods for Optimization of Machining Process Parameters*, International Journal of Modern Manufacturing Technologies, ISSN 2067-3604, IX(1), 17-22.

Received: June 25, 2018 / Accepted: June 15, 2019 / Paper available online: June 20, 2019